### Title
The influence of obliquity in the early Holocene Asian summer monsoon




### Journal
Geophysical Research Letters, 43(9)

### ISSN
0094-8276



### Authors
Wu, Chi-Hua
Lee, Shih-Yu
Chiang, John CH
et al.



### Publication Date
2016-05-16

### DOI
10.1002/2016gl068481

Peer reviewed

AGU PUBLICATIONS

Geophysical Research Letters

RESEARCH LETTER
10.1002/2016GL068481

**Key Points:**
- Asian and North Pacific highs are affected by subtropical heating changes responding to obliquity
- High obliquity augments precessional impact by shifting Holocene Asian monsoon north than today
- Obliquity is responsible also for monsoon changes conventionally thought to be caused by precession

**Correspondence to:**
C.-H. Wu,
chhwu@gate.sinica.edu.tw

**Citation:**
Wu, C.-H., S.-Y. Lee, J. C. H. Chiang, and H.-H. Hsu (2016), The influence of obliquity in the early Holocene Asian summer monsoon, *Geophys. Res. Lett.*, *43*, 4524–4530, doi:10.1002/2016GL068481.

Received 5 JAN 2016
Accepted 19 APR 2016
Accepted article online 20 APR 2016
Published online 4 MAY 2016



# The influence of obliquity in the early Holocene Asian summer monsoon

**Chi-Hua Wu[1], Shih-Yu Lee[1], John C. H. Chiang[2], and Huang-Hsiung Hsu[1]**

[1]Research Center for Environmental Changes, Academia Sinica, Taipei, Taiwan, [2]Department of Geography and Berkeley Atmospheric Sciences Center, University of California, Berkeley, California, USA

**Abstract** The early Holocene climatic optimum is associated with perihelion precession and high obliquity, though most studies emphasize the former over the latter. Asian monsoon proxy records only decisively show the precessional impact. To explore the obliquity effect, four climate simulations are conducted by fixing orbital parameters of present-day (0K), early Holocene (11K), the lowest obliquity (31K), and 11K's precession and eccentricity with 31K's obliquity (11Kp31Ko). We show that high obliquity significantly augments the precessional impact by shifting the Asian monsoon farther north than present. By contrast, the present-day monsoon seasonality can still be identified in the simulations with low obliquity. We argue that the upper tropospheric (South Asian) and lower tropospheric (North Pacific) high-pressure systems are affected by the subtropical atmospheric heating changes responding to obliquity. As a consequence, associated with the changes in meridional gradients of geopotential height and temperature made by the heating, midlatitude transient eddies and monsoon-midlatitude interactions are modulated.

## 1. Introduction

Data and modeling studies have previously revealed substantial effects of the obliquity and precession, individually or combined, on the orbital timing of some major monsoons [*Braconnot and Marti*, 2003; *Caley et al*., 2011; *Chiang et al*., 2015; *Jiang et al*., 2013; *Rossignol-Strick*, 1983; *Wyrwoll et al*., 2007]. The direct effect of obliquity changes to tropical insolation is small, and the associated monsoonal changes are thought to be tied to meridional temperature gradient changes forced from higher latitudes [*Lee and Poulsen*, 2009; *Lourens et al*., 2010]. By contrast, mechanisms of precessional forcing on paleomonsoons appear more apparent and straightforward, e.g., the spatial and temporal characteristics of the Holocene optimum precipitation as a precession paradigm in some monsoon regions—intensity of monsoon during the perihelion precession approximately every 23,000 years [*Cheng et al*., 2012; *Jin et al*., 2014; *Mantsis et al*., 2013; *Nagashima et al*., 2013; *Wu et al*., 2015].

*Wu et al*. [2015] explored the Asian summer monsoon of the early Holocene by investigating climate simulation with orbital parameters set to 11 ka B.P. They show that the high summer insolation strengthens the upper tropospheric South Asian high and lower tropospheric North Pacific high—subtropical high-pressure systems, both of which are dominant controls of the Asian summer monsoon. As a consequence, the summer monsoon subsystems in East and South Asia are stronger and penetrate farther north, and the monsoon trough over the subtropical western North Pacific disappears. While the extremely warm summer climate 11 ka B.P. is commonly attributed to precessional forcing, it was also the time of high obliquity. It raises the question of how high obliquity contributes to the early Holocene Asian monsoon peak.

Recent works have reemphasized the combined effects of precessional and obliquity forcing on the Africa monsoon [*Tuenter et al*., 2003], the Australia monsoon [*Wyrwoll et al*., 2007], and the Asian monsoon also [*Caley et al*., 2011]. Obliquity introduces major changes in the meridional temperature gradient and geopotential height in the subtropical region, which in turn affects the seasonal evolution of the South Asian high and North Pacific high. In light of the potential regulation of the subtropical high-pressure systems on the monsoons in South Asia, Southeast Asia, and the East Asian-western North Pacific (EAWNP) region as shown in *Wu et al*. [2015], this study was motivated by exploring the obliquity impact on the regional monsoons and their interaction.

In this study, we follow on from the simulations in *Wu et al*. [2015] by exploring the effect of obliquity during precessionally-induced peak Northern Hemisphere insolation phases on the Asian monsoon (hereafter, we refer to this precessional phase as "peak northern summer precessional phase"). The model experiments

**Table 1.** Orbital Parameters (Eccentricity, Precession, and Obliquity) in the CAM/SOM Experimental Simulations

| Experiments | E | P | O | Note |
|---|---|---|---|---|
| 0K | 0.016708 | 102.72 | 23.44 | Present-day conditions |
| 11K | 0.019525 | 279.06 | 24.20 | Perihelion precession and high obliquity (11 ka B.P.) |
| 11Kp31Ko | 0.019525 | 279.06 | 22.28 | Sensitivity to the impact of obliquity (compared to 11K) |
| 31K | 0.016087 | 311.88 | 22.28 | Nearly perihelion precession and low obliquity (31 ka B.P.) |

are described in section 2. Section 3 investigates the seasonal and regional characteristics of the monsoon in the four simulations, and section 4 gives concluding remarks.

## 2. Model Experiments

The Community Atmospheric Model (CAM) version 5.1 of the National Center for Atmospheric Research (NCAR) coupled with the slab ocean model (SOM) (http://www.cesm.ucar.edu) is used for exploring the orbital impact. The CAM/SOM simulations were integrated using the finite volume dynamical core at a horizontal resolution of approximately 1°, with the boundary and initial conditions adopted from the Community Earth System Model (CESM) preindustrial control experiment [*Vertenstein et al*., 2010].

The simulation with early Holocene orbital conditions was performed using orbital parameters of 11 ka B.P. (hereafter 11K simulation), and other boundary conditions were kept the same as present-day conditions (refer to *Wu et al*. [2015]). To explore the impact of obliquity, a simulation with the orbital parameters same as 11K simulation except a low obliquity of 22.28° was conducted (11Kp31Ko simulation). We also perform a "real" case (31K simulation) which has the obliquity of 22.28° and a nearly perihelion precession. These simulations are the same except their orbital parameters as shown in Table 1. The integration length of the simulations was 40 years, and the outputs for years 21–40 were analyzed.

## 3. Perihelion Summer Asian Monsoon at High and Low Obliquity

Figure 1 shows the insolation (zonal mean) comparisons among the four orbital configurations. The direct effect of obliquity changes to high latitudes is large (Figure 1b), and apparently, the obliquity is the major cause of the largest insolation difference between 11K and 31K simulations (Figures 1b and 1c).

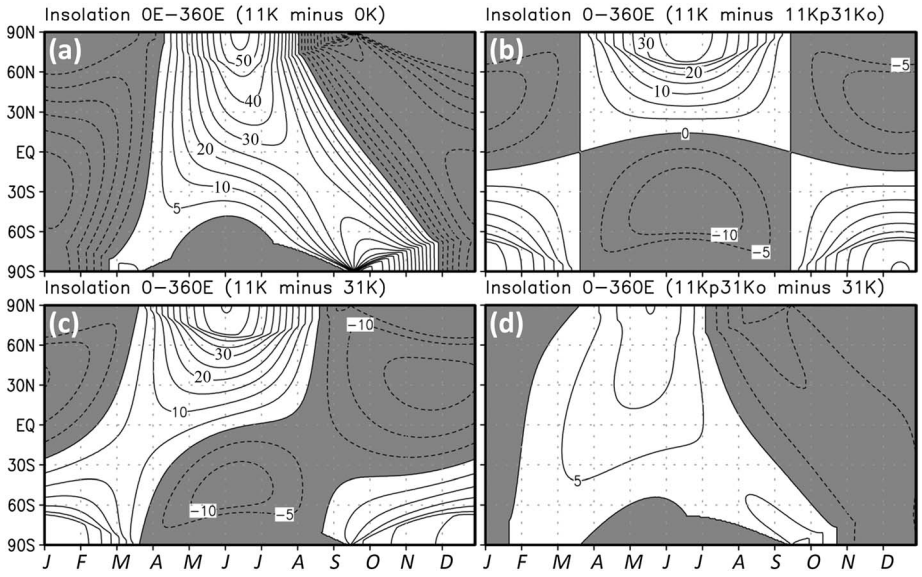


**Figure 1.** Latitude-time distribution of global solar insolation (W $m^{-2}$) for (a) 11K minus 0K, (b) 11K minus 11Kp31Ko, (c) 11K minus 31K, and (d) 11Kp31Ko minus 31K simulations. Negative values are shaded.

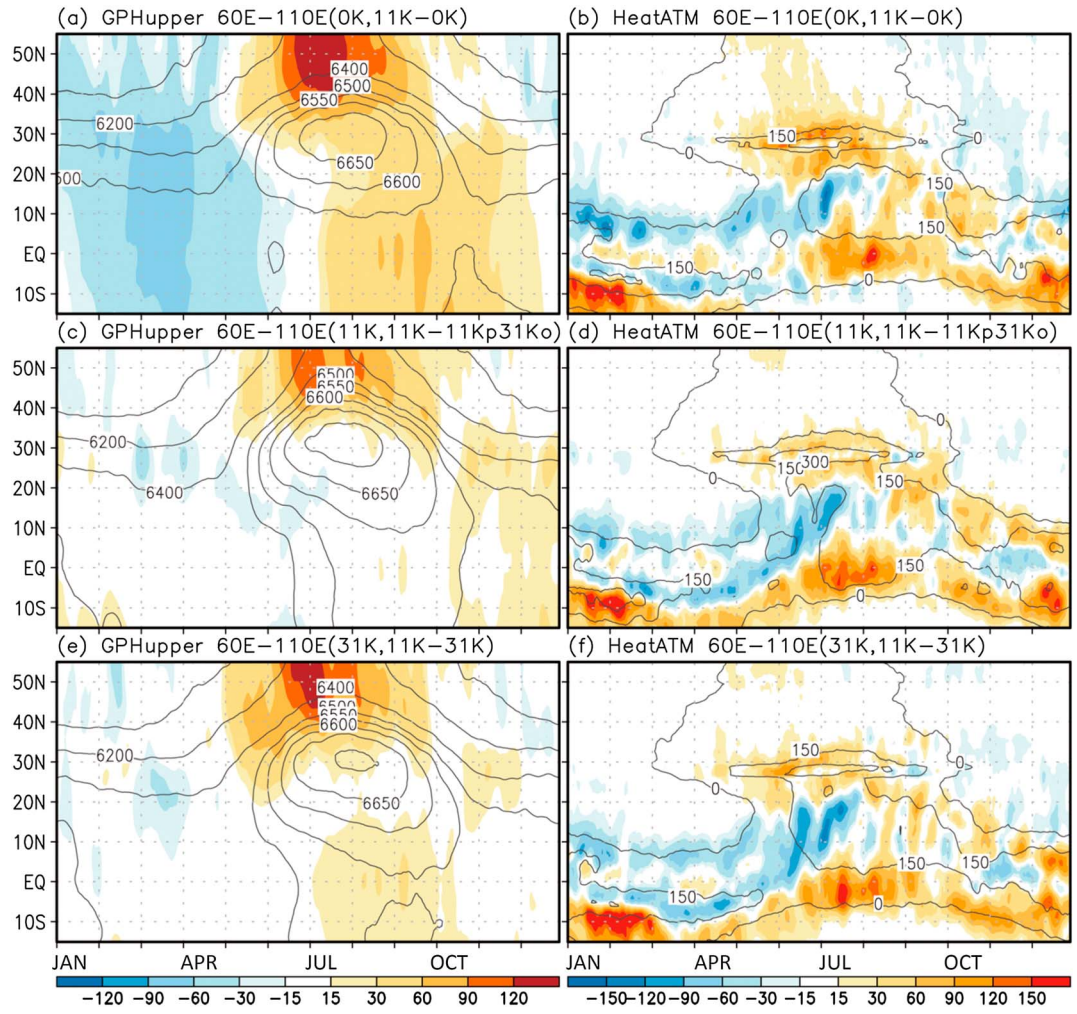


**Figure 2.** Latitude-time plots of (a, c, and e) geopotential height thickness between 200 hPa and 500 hPa (gpm) and (b, d, and f) total column heating of the atmosphere contributed by radiation, precipitation, and surface sensible heat (W $m^{-2}$) in the longitudinal band (60°E–110°E); contour lines/color shadings denote 0K/11K minus 0K simulation (Figures 2a and 2b) , 11K/11K minus 11Kp31Ko simulation (Figures 2c and 2d) , and 31K/11K minus 31K simulation (Figures 2e and 2f).

As will be demonstrated as follows, the obliquity-modulated heating contrast substantially affects the monsoon circulation.

1. South Asia

To identify the atmospheric response to the distinct orbital forcing, Figure 2 shows the upper level geopotential thickness between 500 hPa and 200 hPa and atmospheric column-integrated diabatic heating (sum of precipitation, sensible heat, and radiation). A general feature associated with the South Asian summer monsoon is that strong atmospheric diabatic heating supports the deepening of the upper troposphere (contour lines, Figures 2a and 2b); this corresponds to the development of the South Asian high centered around 20°N–30°N. With higher 11 ka B.P. northern summer insolation, the diabatic heating in summer is greatly increased in 20°N–35°N and the equatorial region but decreased in 5°N–20°N (Figure 2b). The strengthening and expansion of the high pressure in the upper troposphere (contour lines, Figure 2c) closely follows the heating changes (Figures 2a and 2b).The difference in the response between the 11K and 11Kp31Ko simulations (Figures 2c and 2d) provides a measure of the contribution to obliquity in the above changes. The northward shift and strengthening of the South Asian high and the heating changes are overall in phase with the impact of peak northern summer precessional phase. Under low obliquity, this precessional impact is considerably reduced (Figures 2e and 2f). We furthermore quantify changes to the monsoon strength by gauging the

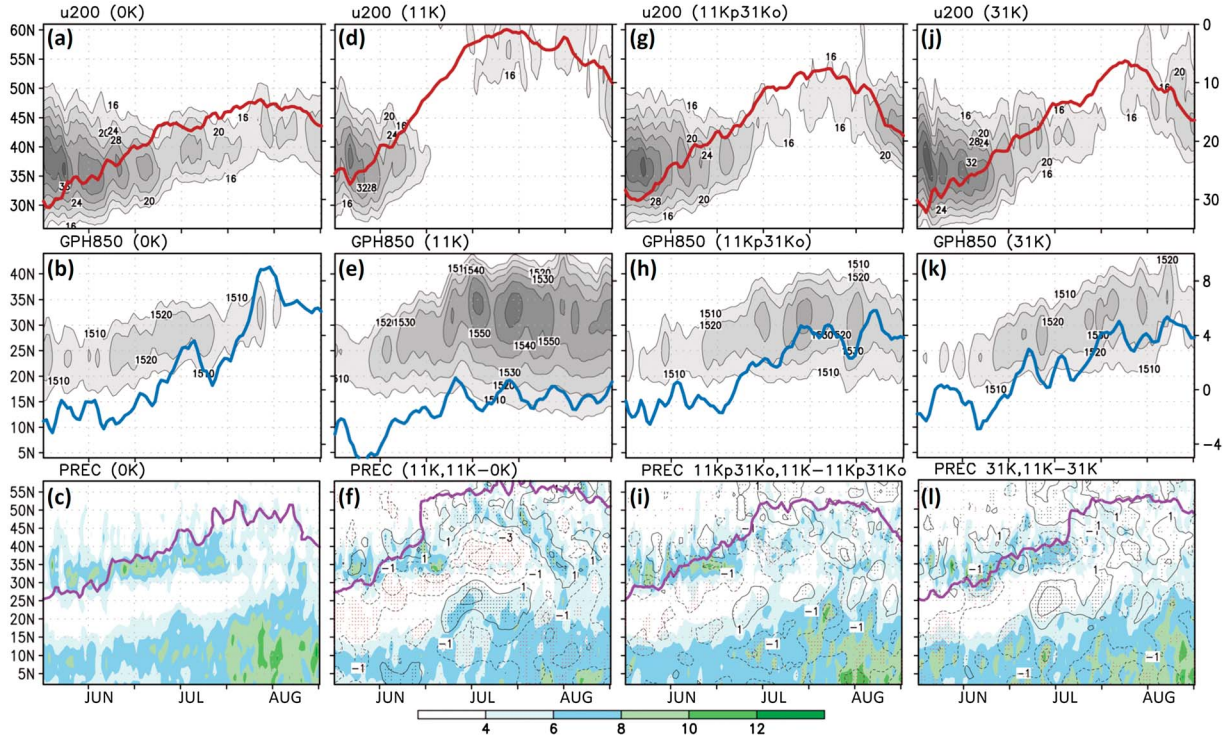


**Figure 3.** Latitude-time cross sections of (a) 200 hPa zonal wind speed (m $s^{-1}$) in 110°E–140°E, (b) 850 hPa geopotential height (gpm) in 130°E–150°E, and (c) precipitation (mm $d^{-1}$) 130°E–150°E of 0K simulation. (d–f)/(g–i)/(j–l) Same as Figures 3a–3c except that they show 11K/11Kp31Ko/31K simulations. Red lines denote the 200 hPa zonal wind speed in region (110°E–140°E, 30°N–50°N). Blue lines denote the western North Pacific monsoon strength quantified by the difference in the 850 hPa westerlies between regions (100°E–130°E, 5°N–15°N) and (110°E–140°E, 20°N–30°N) [*Wang and Fan*, 1999]. Purple lines denote the latitude where the equivalent potential temperature ($\theta_e$) at 850 hPa averaged over 130°E–140°E is equal to 330 K (gaging the end of Baiu season) [*Suzuki and Hoskins*, 2009]. Right side coordinates are for the indices. The contour lines denote precipitation difference with 90% confidence level (dots) for 11K minus 0K (Figure 3f), 11K minus 11Kp31Ko (Figure 3i) , and 11K minus 31K simulations (Figure 3l).

meridional contrast in upper level geopotential depth (500 hPa–200 hPa) between regions (60°E–110°E, 20°N–40°N) and (60°E–110°E, 10°S–10°N), similar to *Sun et al.* [2010]. The simulated monsoon strengths in mid-June of South Asia are 80 m (0K), 123 m (11K), 102 m (11Kp31Ko), and 78 m (31K). Comparison between these simulations indicates that the increased meridional thermal contrast over the South Asian summer monsoon region during 11K (54% from 0K to 11K) is cut by half (28% from 0K to 11Kp31Ko) under the influence of low obliquity. Furthermore, even with the influence of high precessional insolation in 31K, because of the low obliquity, that monsoon may have been weaker than today.

2. East Asia and western North Pacific

The monsoon changes between the simulations are also considerable over the EAWNP region (Figure 3). Under high northern summer insolation (11K simulation), the midlatitude upper tropospheric jet stream weakens (Figure 3d), the North Pacific high strengthens and expands southward and northward (Figure 3e), the onset and retreat of Meiyu-Baiu occurs earlier (Figure 3f), and the western North Pacific monsoon trough disappears as a consequence of the stronger North Pacific high (Figure 3e). These monsoonal changes have been elaborated in *Wu et al.* [2015]. Regardless of the 31K precessional forcing, the present-day characteristics of the upper level jet stream, the lower level North Pacific subtropical high, and the Meiyu-Baiu rain band are apparent in the 11Kp31Ko and 31K simulations, particularly in the 31K simulation and in the early summer (late May to early July) (Figures 3g–3l). The simulated monsoonal changes from 0K to 11K is cut under the influence of low obliquity.

Since obliquity-induced heating changes exhibit large spatial variability in the Tropics (e.g., Figures 2d–2f), the northern South Asian region (NSA, 60°E–110°E, 20°N–35°N) and southern South Asian region (SSA, 60°E–110°E, 5°N–20°N) are discussed separately. In the NSA region, the candle-like heating [*Chen et al.*, 2014] associated with diabatic heating over the foothills of southern Tibetan Plateau-Himalayas is a dominant

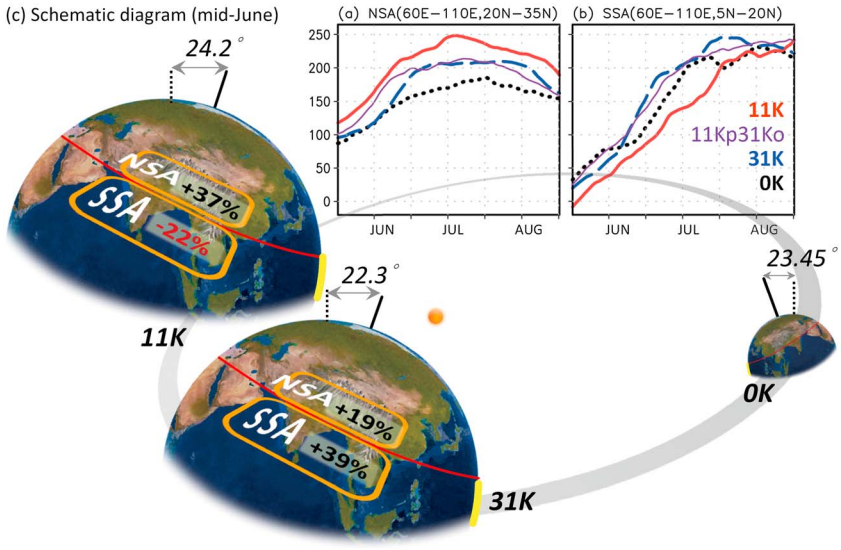


**Figure 4.** Seasonal evolution of total column heating of the atmosphere ($W\,m^{-2}$) in the (a) northern South Asian region (60°E–110°E, 20°N–35°N, NSA) and (b) southern South Asian region (60°E–110°E, 5°N–20°N, SSA); black dot lines for 0K, red solid lines for 11K, purple solid line for 11Kp31Ko, and blue dashed lines for 31K simulations. (c) Schematic diagram of the heating changes (relative to 0K) in mid-June.

contribution. In the SSA region, the heating is related to the penetration of convection and precipitation under the influence of the south-north oriented mesoscale mountain ranges.

The present-day Asian summer monsoon reaches its peak season starting in mid-June. We therefore simplify the discussion by focusing on the mid-June heating changes. In the NSA region, the diabatic heating in mid-June increases by 37% (from 157 to 215 $W\,m^{-2}$) in the 11K simulation and 19% (from 157 to 187 $W\,m^{-2}$) in the 31K simulation from present day (Figure 4a). Under the influence of precession, the atmospheric heating in the NSA region is increased by ~20% compared to present. The major impact of the obliquity is found in the SSA region. In mid-June of peak northern summer precessional phase, the heating over here decreases by 22% (from 109 to 85 $W\,m^{-2}$) at high obliquity (11K simulation) but greatly increases by 39% (from 109 to 152 $W\,m^{-2}$) at low obliquity (31K simulation), when compared to the present. A summary of the mid-June heating change in 11K and 31K simulations is shown in Figure 4c.

We reemphasize that the major monsoon features in June of 31K and 0K simulations are similar to a certain extent (Figure 3), as are the heating structures shown in Figure 2. Based on the similarity, we argue that the increase of the atmospheric heating in the SSA region, as a result of low obliquity, critically confines the subtropical high-pressure systems. The 11K forcing-induced expansion of the North Pacific high as shown in *Wu et al.* [2015] is greatly weakened. The perihelion precession-induced monsoon changes are partly canceled as a consequence. In global scale, low obliquity causes stronger meridional temperature gradients that would favor greater midlatitude eddies and poleward heat transport [*Mantsis et al.*, 2014], and vice versa. At low obliquity (31K simulation), the atmospheric heating of South Asia (mean of NSA and SSA regions) is much higher than that at high obliquity (11K simulation) by 40 $W\,m^{-2}$ in mid-June. The meridional heating gradient is enlarged, with more active midlatitude eddies, in the 31K relative to 11K simulation.

## 4. Concluding Remarks

This study addresses the role of high obliquity in the early Holocene (11 ka BP) Asian summer monsoon. The East and South Asian monsoons were thought to penetrate farther north than present day, whereas in the western North Pacific the monsoon trough disappears. High-resolution speleothem monsoon records, in particular from China, show a clear precessional timing of the Asian monsoon intensity as well as hydrologic processes (e.g., moisture transport in South Asia). Nevertheless, newly inquired tropical Pacific precipitation records challenge the precession paradigm by showing both precession and obliquity signals and whose

influences were also seen in model simulations [*Liu et al*., 2015]. Due to the great influence of precession on seasonal insolation, it was conventionally thought that monsoonal climate variations mainly responded to precessional forcing. By investigating CAM/SOM-simulated perihelion summer Asian monsoon with high and low obliquity, both real (11K and 31K simulations) and sensitivity (11Kp31Ko simulation) cases, we argue that obliquity forcing could be responsible also decisively for the monsoon changes and provide further support to the precipitation response in obliquity band.

During peak northern summer precessional phase with high obliquity (11K simulation), the massive heating of the Asian continent becomes much higher than its present-day condition. In the southern Tibetan Plateau and Northeast Asia (not shown by the figure), where the atmospheric diabatic heating is closely related to the exact timing of the summer monsoon subseasonality, the mid-June heating increases by approximately 40% relative to present day. Even at low obliquity (31K simulation), the enhanced heating over the two regions still occurs by approximately 20%, indicating a dominant effect of the perihelion precession.

Nevertheless, compared with the heating response between the two extreme obliquity conditions, the heating of the southern South Asian region (5°N–20°N, SSA region) is reduced by approximately 20% at the high obliquity but enhanced by approximately 40% at the low obliquity. The overall heating over South Asia is greatly increased in the 31K simulation relative to 11K simulation; larger meridional gradients of geopotential height and temperature made are related to the reduced heating over the NSA region and enhanced heating over the SSA region because of low obliquity (Figure 4c).

It is likely that the great enhancement of the heating in the SSA region, as a result of low obliquity, cancels part of the peak northern summer precession effects on the monsoon. Unlike in the 11K simulation, the EAWNP monsoon behavior in the 31K simulation resembles more closely to the present, in particular in the early summer. In the 11K simulation, the overall stronger land-ocean heating contrast results in the stronger upper level South Asian high and lower level North Pacific high, as well as the weaker meridional gradients and the much weaker East Asian upper level jet stream. The western North Pacific lower level monsoon trough disappears as a consequence. Also in the perihelion summer but at low obliquity, the major monsoon circulations in the 31K simulation are simulated more closely to the present. The western North Pacific monsoon trough can be identified albeit at weaker strength. The onset of the western North Pacific monsoon in the 31K simulation corresponds to the gradual weakening of the midlatitude upper level jet stream in July. More poleward heat transport induced by lower obliquity is consistent with previous suggestion [*Mantsis et al*., 2014]. The modeling result in *Chen et al*. [2010] also indicated the obliquity effect on modulating the intrinsic dynamical mode during the EAWNP summer monsoon, suggesting the Pacific-Japan-pattern dynamics [*Kosaka and Nakamura*, 2006; *Nitta*, 1987]. On the other hand, the limitation exists in the comparison between paleodata and our simulations because of present-day boundary condition. *Weber and Tuenter* [2011] indicated the role of ice sheet and greenhouse gases in modulating the orbital control of the monsoon. Although the impact of the coupled ice sheet and greenhouse gas changes might be overestimated due to their nonlinear response to orbital effects [*Sun et al*., 2015; *Yin and Berger*, 2011], it is worthy of further investigation to explore how including these paleoforcings would affect the orbital controls.

**Acknowledgments**

This work was supported by the Consortium for Climate Change Study (CCliCS) under the auspices of the Ministry of Science and Technology (MOST), Taiwan, under grant NSC 100–2119–M–001–029–MY5 (H.H.H. and C.H.W.) and MOST 104–2111–M–001–001 (C.H.W.). S.Y.L. was supported by MOST grants 102–2111–M–001–002–MY3, 104–2119–M–002–003, and 104–2611–M–001–001. J.C. was supported by NSF grant AGS–1405479. We are grateful for the models CESM (http://www.cesm.ucar.edu) of the National Center for Atmospheric Research (NCAR). Location of the simulations is currently on the CCliCS database (http://cclics.rcec.sinica.edu.tw). We also thank the anonymous reviewers for their constructive comments and Hai-Wei Lin for preparing schematic diagram.

## References

Braconnot, P., and O. Marti (2003), Impact of precession on monsoon characteristics from coupled ocean atmosphere experiments: Changes in Indian monsoon and Indian Ocean climatology, *Mar. Geol.*, *201*(1–3), 23–34.

Caley, T., B. Malaize, M. Revel, E. Ducassou, K. Wainer, M. Ibrahim, D. Shoeaib, S. Migeon, and V. Marieu (2011), Orbital timing of the Indian, East Asian and African boreal monsoons and the concept of a "global monsoon", *Quat. Sci. Rev.*, *30*(25–26), 3705–3715.

Chen, G. S., Z. Liu, and J. E. Kutzbach (2014), Reexamining the barrier effect of the Tibetan Plateau on the South Asian summer monsoon, *Clim. Past*, *10*(3), 1269–1275.

Chen, G.-S., Z. Liu, S. C. Clemens, W. L. Prell, and X. Liu (2010), Modeling the time-dependent response of the Asian summer monsoon to obliquity forcing in a coupled GCM: A PHASEMAP sensitivity experiment, *Clim. Dyn.*, *36*(3–4), 695–710.

Cheng, H., A. Sinha, X. F. Wang, F. W. Cruz, and R. L. Edwards (2012), The Global Paleomonsoon as seen through speleothem records from Asia and the Americas, *Clim. Dyn.*, *39*(5), 1045–1062.

Chiang, J. C. H., I. Y. Fung, C. H. Wu, Y. H. Cai, J. P. Edman, Y. W. Liu, J. A. Day, T. Bhattacharya, Y. Mondal, and C. A. Labrousse (2015), Role of seasonal transitions and westerly jets in East Asian paleoclimate, *Quat. Sci. Rev.*, *108*, 111–129.

Jiang, D. B., X. M. Lang, Z. P. Tian, and L. X. Ju (2013), Mid-Holocene East Asian summer monsoon strengthening: Insights from Paleoclimate Modeling Intercomparison Project (PMIP) simulations, *Palaeogeogr. Palaeoclimatol. Palaeoecol.*, *369*, 422–429.

Jin, L., B. Schneider, W. Park, M. Latif, V. Khon, and X. Zhang (2014), The spatial–temporal patterns of Asian summer monsoon precipitation in response to Holocene insolation change: A model-data synthesis, *Quat. Sci. Rev.*, *85*, 47–62.

Kosaka, Y., and H. Nakamura (2006), Structure and dynamics of the summertime Pacific–Japan teleconnection pattern, *Q. J. R. Meteorol. Soc.*, *132*(619), 2009–2030.
Lee, S. Y., and C. J. Poulsen (2009), Obliquity and precessional forcing of continental snow fall and melt: Implications for orbital forcing of Pleistocene ice ages, *Quat. Sci. Rev.*, *28*(25–26), 2663–2674.
Liu, Y., et al. (2015), Obliquity pacing of the western Pacific Intertropical Convergence Zone over the past 282,000 years, *Nat. Commun.*, *6*, 10018, doi:10.1038/ncomms10018.
Lourens, L. J., J. Becker, R. Bintanja, F. J. Hilgen, E. Tuenter, R. S. W. van de Wal, and M. Ziegler (2010), Linear and non-linear response of late Neogene glacial cycles to obliquity forcing and implications for the Milankovitch theory, *Quat. Sci. Rev.*, *29*(1–2), 352–365.
Mantsis, D. F., A. C. Clement, B. Kirtman, A. J. Broccoli, and M. P. Erb (2013), Precessional cycles and their influence on the North Pacific and North Atlantic summer anticyclones, *J. Clim.*, *26*(13), 4596–4611.
Mantsis, D. F., B. R. Lintner, A. J. Broccoli, M. P. Erb, A. C. Clement, and H. S. Park (2014), The response of large-scale circulation to obliquity-induced changes in meridional heating gradients, *J. Clim.*, *27*(14), 5504–5516.
Nagashima, K., R. Tada, and S. Toyoda (2013), Westerly jet-East Asian summer monsoon connection during the Holocene, *Geochem. Geophys. Geosyst.*, *14*, 5041–5053, doi:10.1002/2013GC004931.
Nitta, T. (1987), Convective activities in the tropical western Pacific and their impact on the Northern Hemisphere summer circulation, *J. Meteorol. Soc. Jpn.*, *65*(3), 373–390.
Rossignol-Strick, M. (1983), African monsoons, an immediate climate response to orbital insolation, *Nature*, *304*(5921), 46–49.
Sun, Y., Y. H. Ding, and A. G. Dai (2010), Changing links between South Asian summer monsoon circulation and tropospheric land-sea thermal contrasts under a warming scenario, *Geophys. Res. Lett.*, *37*, L02704, doi:10.1029/2009GL041662.
Sun, Y. B., et al. (2015), Astronomical and glacial forcing of East Asian summer monsoon variability, *Quat. Sci. Rev.*, *115*, 132–142.
Suzuki, S., and B. Hoskins (2009), The large-scale circulation change at the end of the Baiu season in Japan as seen in ERA40 data, *J. Meteorol. Soc. Jpn.*, *87*(1), 83–99.
Tuenter, E., S. L. Weber, F. J. Hilgen, and L. J. Lourens (2003), The response of the African summer monsoon to remote and local forcing due to precession and obliquity, *Global Planet. Change*, *36*(4), 219–235.
Vertenstein, M., T. Craig,, A. Middleton, D. Feddema, and C. Fischer (2010), CESM1.0.3 User's Guide. [Available at http://www.cesm.ucar.edu/.]
Wang, B., and Z. Fan (1999), Choice of South Asian summer monsoon indices, *Bull. Am. Meteorol. Soc.*, *80*(4), 629–638.
Weber, S. L., and E. Tuenter (2011), The impact of varying ice sheets and greenhouse gases on the intensity and timing of boreal summer monsoons, *Quat. Sci. Rev.*, *30*(3–4), 469–479.
Wu, C.-H., J. C. H. Chiang, H.-H. Hsu, and S.-Y. Lee (2015), Orbital control of the western North Pacific summer monsoon, *Clim. Dyn.*, *46*(3–4), 897–911.
Wyrwoll, K. H., Z. Y. S. Liu, G. Chen, J. E. Kutzbach, and X. D. Liu (2007), Sensitivity of the Australian summer monsoon to tilt and precession forcing, *Quat. Sci. Rev.*, *26*(25–28), 3043–3057.
Yin, Q. Z., and A. Berger (2011), Individual contribution of insolation and $CO_2$ to the interglacial climates of the past 800,000 years, *Clim. Dyn.*, *38*(3–4), 709–724.